The Prostate

WILEY

The Prostate

ORIGINAL ARTICLE OPEN ACCESS

The Role of Dynamic Contrast Enhanced Magnetic Resonance Imaging in Evaluating Prostate Adenocarcinoma: A Partially-Blinded Retrospective Study of a Prostatectomy Patient Cohort With Whole Gland Histopathology Correlation and Application of PI-RADS or TNM Staging

Sajeev Sridhar[1] | Zeyad Abouelfetouh[1] | Ion Codreanu[2] | Nakul Gupta[3] | Shu Zhang[1] | Eleni Efstathiou[4] | Daniel K. Karolyi[5] | Steven S. Shen[6] | Peter S. LaViolette[7] | Brian Miles[8] | Diego R. Martin[6]

[1]Department of Radiology, Houston Methodist Research Institute, Houston, Texas, USA | [2]Department of Radiology, Houston Methodist Research Institute, Nicolae Testemițanu State University of Medicine and Pharmacy, Chișinău, Moldova | [3]Department of Radiology, Houston Methodist Hospital, Houston Methodist Research Institute, Houston Radiology Associated, Houston, Texas, USA | [4]Department of Medicine, Houston Methodist Hospital, Houston Methodist Oncology Partners, Houston, Texas, USA | [5]Department of Radiology, Virginia Tech Carilion School of Medicine, Roanoke, Virginia, USA | [6]Department of Pathology, Houston Methodist Hospital, Houston Methodist Research Institute, Houston, Texas, USA | [7]Department of Radiology, Medical College of Wisconsin, Milwaukee, Wisconsin, USA | [8]Department of Urology, Houston Methodist Hospital, Houston Methodist Urology Associates, Houston, Texas, USA

Correspondence: Diego R. Martin (drmartin@houstonmethodist.org)

Received: 9 September 2024 | **Accepted:** 11 November 2024

Funding: This research was supported by the NIH 1R01CA245920-02. MD Anderson Foundation. Houston Methodist Neal Cancer Center.

Keywords: ADC | conspicuity | DCE | DWI | MRI | PI-RADS | prostate cancer | T2W

ABSTRACT

Background: Dynamic contrast-enhanced (DCE) magnetic resonance imaging (MRI) in the current Prostate Imaging-Reporting and Data System version 2.1 (PI-RADS v2.1) is considered optional, with primary scoring based on T2-weighted imaging (T2WI) and diffusion weighted imaging (DWI). Our study is designed to assess the relative contribution of DCE MRI in a patient-cohort with whole mount prostate histopathology and spatially-mapped prostate adenocarcinoma (PCa) for reference.

Methods: We performed a partially-blinded retrospective review of 47 prostatectomy patients with recent multi-parametric MRI (mpMRI). Scans included T2WI, DWI with apparent diffusion coefficient (ADC) mapping, and DCE imaging. Lesion conspicuity was scored on a 10-point scale with ≥ 6 considered "positive," and image quality was assessed on a 4-point scale for each sequence. The diagnostic contribution of DCE images was evaluated on a 4-point scale. The mpMRI studies were assigned PI-RADS scores and tumor, node, metastasis (TNM) T-stage with blinded comparison to spatially-mapped whole-mount pathology. Results were compared to the prospective clinical reports, which used standardized PI-RADS templates that emphasize T2WI, DWI and ADC.

Results: Per lesion sensitivity for PCa was 93.5%, 82.6%, 63.0%, and 58.7% on T2WI, DCE, ADC and DWI, respectively. Mean lesion conspicuity was 8.5, 7.9, 6.2, and 6.1, on T2W, DCE, ADC and DWI, respectively. The higher values on T2WI and DCE imaging were not significantly different from each other but were both significantly different from DWI and

Abbreviations: ACR, American College of Radiology; ADC, apparent diffusion coefficient; DCE, dynamic contrast enhanced; DWI, diffusion-weighted imaging; mpMRI, multiparametric magnetic resonance imaging; PCa, prostate adenocarcinoma; PI-RADS, prostate imaging-reporting and data system; T1W, T1 weighted; T2W, T2 weighted.

This is an open access article under the terms of the Creative Commons Attribution-NonCommercial License, which permits use, distribution and reproduction in any medium, provided the original work is properly cited and is not used for commercial purposes.

© 2024 The Author(s). *The Prostate* published by Wiley Periodicals LLC.

ADC ($p < 0.001$). DCE scans were determined to have a marked diagnostic contribution in 83% of patients, with the most common diagnostic yield being detection of contralateral peripheral zone tumor or delineating presence/absence of extra-prostatic extension (EPE), contributing to more accurate PCa staging by PI-RADS or TNM, as compared to histopathology. **Conclusion:** We demonstrate that DCE may contribute to lesion detection and local staging as compared to T2WI plus DWI-ADC alone and that lesion conspicuity using DCE is markedly improved as compared to DWI-ADC. These findings support modification of PI-RADS v2.1 to include use of DCE acquisitions and that a TNM staging is feasible on mpMRI as compared to surgical pathology.

1 | Introduction

The importance of multiparametric magnetic resonance imaging (mpMRI) of prostate adenocarcinoma (PCa) is well-recognized in diagnosis, directing biopsies, and therapy management [1–7]. There remains a focus on continued validation and development of improved strategies for standardized image acquisitions, image processing, analysis, and reporting.

The Prostate Imaging-Reporting and Data System (PI-RADS), version 2.1 (v2.1) was published in 2019 and developed by an internationally representative group involving the American College of Radiology (ACR), European Society of Urogenital Radiology (ESUR), and AdMeTech Foundation [4]. This document specifies basic technical requirements of mpMRI, as well las a standardized reporting nomenclature. Changes to v2.1 from prior versions includes differentiating peripheral (PZ) from transition zone (TZ) tumors, primarily relying on diffusion weighted imaging (DWI) in the PZ and T2-weighted imaging (T2WI) in the TZ. PI-RADS attributes a supportive role for Dynamic contrast-enhanced (DCE) T1-weighted (T1W) images, with some centers advocating no longer including these acquisitions [8–14].

Support for DCE magnetic resonance imaging (DCE MRI) has come from various types of PCa studies. DCE MRI has been used to assess tissue perfusion and permeability and to show that PCa may have differentiated enhancement kinetics with faster enhancement and earlier contrast washout, as compared with nonmalignant prostate [6, 15]. Direct comparison of contrast-enhanced ultrasound and DCE MRI showed a superior performance of DCE MRI for detection and for predicting aggressiveness [16]. DCE MRI has been shown to improve confidence of tumor detection for less-experienced readers [17, 18]. In comparison, DWI generally remains signal-limited, noisy, and low resolution, even with two or more minutes of acquisition time. DWI, and the calculated ADC map images, are sensitive to several sources of artifacts, including motion, bowel gas and metal in patients with surgical clips or hip prostheses [19–23].

Since the introduction of PI-RADS there has been a growing body of evidence for the diagnostic value of DCE in PCa detection and staging [15, 24–29]. Overall image quality of T2WI, DWI and DCE-T1W images continue to evolve, each on their own paths of development. It stands to reason that there is need for continued assessment of the relative contributions of each of these acquisitions in relation to objective measures of tumor defined by histopathology.

Our objective is to assess the relative sensitivity and diagnostic contributions of DCE MRI in a well-defined cohort of PCa patients with surgical pathology, providing the opportunity for evaluation of spatially mapped histopathology as a standard of reference, and for evaluation of the capacity of DCE-T1W imaging to impact PI-RADS or tumor, node, metastasis (TNM) staging.

2 | Methods

2.1 | Study Population and Design

This was an IRB approved, HIPAA compliant, partially-blinded retrospective study with a waiver for informed consent. Data was collected from our Electronic Patient Registry (mPower, Nuance, Burlington, MA), using a search window between July 2018 through December 2022 to derive 50 prostatectomy PCa patients with prior mpMRI (Figure 1).

2.2 | Image Acquisition

mpMRI protocol was based on PI-RADS v2 and 2.1 specifications, the American Urological Association (AUA) guidelines, and a recent review, including gadolinium-enhanced imaging

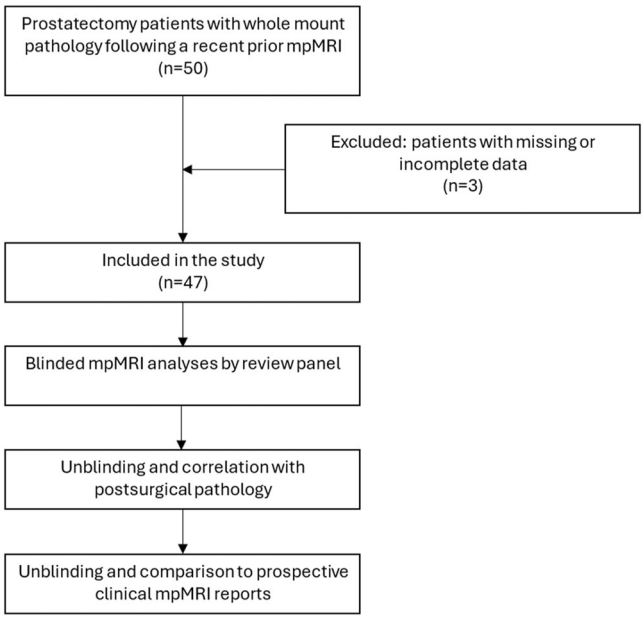

FIGURE 1 | Study Flowchart. mpMRI = multiparametric magnetic resonance imaging.

[1, 4, 30, 31]. Scans were performed at several hospitals of the same health system across five MRI scanners from two vendors: Discovery MR750 3.0 T (GE Healthcare, Waukesha, WI, $n = 29$ patients), Magnetom SKYRA 3.0 T (Siemens Healthcare, Erlangen, Germany, $n = 16$ patients), Optima MR450w 1.5 T (GE Healthcare, Waukesha, WI, $n = 2$ patients), Magnetom AERA 1.5 T (Siemens Healthcare, Erlangen, Germany, $n = 2$ patients) and SIGNA Architect 3.0 T (GE Healthcare, Waukesha, WI, $n = 1$ patient). Scans were obtained using a phased-array surface coil. No endorectal coil was used. Intravenous (IV) Glucagon (1 mg) was administered on the scanner table. Patients were instructed to self-administer a Fleet's enema before their appointment to minimize rectal stool and gas. Standard MRI sequences used T1W imaging, T2WI, and DWI with apparent diffusion coefficient (ADC) maps as well as DCE sequences (Table 1). Pre-contrast T1W images were acquired in axial plane using T1W 3D-gradient echo (GRE) technique. T2W images were acquired in sagittal, oblique-axial and oblique-coronal planes using FSE technique. DWI/ADC images were acquired in oblique-axial planes with at least three *b*-values, from which one was ≥ 1400 s/mm^2. Multiphase acquisition with temporal resolution of 5–7 s/scan was used to acquire DCE images in oblique-axial planes post-IV administration of Gadolinium (Gadavist, 0.1 mmol/kg at 3 mL/s, Bayer Pharmaceutical, Whippany, NJ).

2.3 | MRI Evaluation

This was a partially-blinded study with the investigators being aware that all patients had a prostatectomy but blinded to the original radiological reports, and histopathology. Images were reviewed on a picture archiving and communication system (Universal Viewer, GE Healthcare, Chicago, IL) by the clinical investigational team comprised of two Board-certified Radiologists with over 10 and 20 years of mpMRI experience, and two clinical research fellows. Each study was displayed deidentified and reviewed with a standardized protocol, viewing the T2W images first, followed by DWI (from low to high *b*-values), ADC maps and finally DCE images. DCE images were visualized in the axial plane scrolling in the time domain for each axial slice, then incrementing to the next slice to view the perfusion in the time domain. The results were observational looking at abnormal increased arterial phase enhancement in the prostate PZ as a marker of tumor, without quantitative kinetics.

Sensitivity was determined on a per lesion octant anatomic grid of each prostate and compared to whole mount histopathology as reference. Octant PZ spatial mapping followed PI-RADS guidelines [4]. Central and transitional zones were considered central gland (CG) and outlined by the inner prostatic capsule. Lesion conspicuity was scored on a 10-point scale (1-lowest, 10-highest) on T2W, DWI, ADC, and DCE-T1W sequences. Image quality of sequences (T2W, DWI, ADC and DCE-T1W) was evaluated individually on a 4-point scale (1-unreadable, 2-poor, 3-satisfactory, 4-excellent). DCE sequences' contribution towards the final diagnosis was separately evaluated on a 4-point scale (1–lesion(s) not visualized on DCE images, 2–lesion(s) visualized, but DCE had no added value towards the diagnosis, 3–DCE images increased confidence for establishing the diagnosis, 4–DCE images were essential for diagnosis). An overall T-stage was assigned according to the TNM classification.

Investigational findings were compared to the clinical MRI reports. The clinical reports were prospective interpretations generated with a structured template following PI-RADS v2 and v2.1 guidelines. Discrepancies and their causes were documented and tabulated.

2.4 | Histopathology

Histology of total prostatectomy whole mount cross-sectional specimens with hematoxylin eosin (H&E) staining as well as Gleason scoring and TNM staging were assessed as per standards of practice [32–35] by one pathologist with over 20 years of prostate clinical pathology subspecialty experience. All cases had whole mount preparations, as per routine practice at our center. The prostatectomy pathology was collected as part of a prior IRB-approved protocol for a tissue repository at our institution under direction of the lead urologist on this study. Tumor mapping corresponded to the MRI regional mapping, as per recommendations from the AUA [1, 30]. Histopathology records are maintained in a Research Electronic Data Capture database.

2.5 | Statistical Analysis

Sensitivity of MR sequences (T2W, DWI, ADC and DCE-T1W) for detecting PCa lesions was calculated on a per-lesion score with an octant spatial grid of the PZ, or CG, compared against whole mount histopathology. Conspicuity scores on each sequence were compared using Student's *t*-test ($p \leq 0.05 =$ significant), a score of ≥ 6 being considered diagnostic. Pearson's correlation coefficients were calculated, correlating conspicuity scores of different MRI sequences with the Gleason grade found on histopathology and for correlating the ADC values with the Gleason grade. Linear correlation analysis of conspicuity scores on DWI, ADC and DCE-T1W sequences against lesional conspicuity on T2W was performed. A contingency matrix was used to correlate the data obtained by mpMRI and postsurgical pathology results. GraphPad Prism 10 (Dotmatics, Boston, MA) was used for calculations and graphing statistics.

3 | Results

3.1 | Patient Demographics and Group Distribution

A list of 50 male patients who underwent prostatectomy following a mpMRI of the prostate gland was collated by mPower from our electronic database. After exclusions, 47 patients were included in the study (Figure 1). Clinical details and tumor characteristics are summarized in Table 2.

TABLE 1 | Representative MRI parameters by scanner type.

Scanner	Sequence	FOV (mm)	Acquisition matrix	Slice thickness (mm)	Slice spacing (mm)	TR (msec)	TE (msec)	Fat suppression
Siemens SKYRA 3.0T[Z]	AX T2W	180 × 180	320 × 320	3	3	3500	101	No
	AX DWI and ADC *50, 800, 1600*	150 × 73.3	90 × 44	3.5	3.5	5700	83	Yes
	AX DCE-T1W	260 × 260	192 × 154	3.5	3.5	5	2	Variable*
Siemens AERA 1.5 T	AX T2W	180 × 180	320 × 275	3	3	9190	134	No
	AX DWI and ADC *50, 800, 1600*	200 × 200	128 × 128	3	3	8500	70	Yes
	AX DCE-T1W	260 × 260	192 × 154	3.5	3.5	4.12	1.63	Variable*
GE Discovery MR750 3.0T[F]	AX T2W	180 × 170	288 × 256	3	3.3	7322	128	No
	AX DWI and ADC *100, 500, 1000, 1600*[†]	240 × 220	160 × 80	4	4.3	4412	61	Yes
	AX DCE-T1W	240 × 240	224 × 128	4	4	3.51	1.23	Variable*
GE Optima MR450w 1.5T[F]	AX T2W	180 × 180	320 × 224	3	3	3972	104	No
	AX DWI and ADC *50, 800, 1400*	180 × 180	140 × 70	3	3	5206	75	Yes
	AX DCE-T1W	260 × 260	224 × 128	4	4	3.2	1.16	Variable*
GE SIGNA Architect 3.0T[F]	AX T2W	180 × 180	320 × 256	3	3	4562	103	No
	AX DWI *0, 400, 1500*	180 × 180	98 × 64	4	4	5735	81	Yes
	AX DCE-T1W	180 × 180	224 × 128	4	4	4.48	1.42	Variable*

Note: DWI *b*-values (in italics) are shown for the corresponding scanners.
Abbreviations: ADC, apparent diffusion coefficient; AX, axial; DCE-T1W, dynamic contrast-enhanced T1-weighted; DWI, diffusion weighted imaging; FOV, field of view; T2W, T2-weighted; TE, time to echo; TR, repetition time.
*Not all scans evaluated in this cohort have fat suppression, as detailed in the *Image Quality* results.
[†]*b*-value of 1600 was acquired separately.
[Z]Reduced FOV technique ZOOMit was used with this scanner to obtain DWI.
[F]Reduced FOV technique FOCUS was used with these scanners to obtain DWI.

TABLE 2 | Patient characteristics and histopathological details.

Characteristic	Data	
No. of patients	47	
Caucasian (Not Hispanic or Latino)	33	(70.2)
Caucasian (Hispanic or Latino)	3	(6.4)
Black	10	(21.3)
Asian	1	(2.1)
Age (years)*	68	(61–71.5)
Serum PSA (ng/mL)*	7.2	(5–11.6)
PSA density (ng/mL^2)*	0.20	(0.13–0.29)
Time between MRI scan and prostatectomy (weeks)*	12.07	(7.5–19.64)
Prostate volume (mL)*	36	(28.3–48.8)
Prostate weight (g)*	35.5	(27.0–45.5)
Dominant tumor size (cm)*	2.2	(1.6–2.9)
Prostate involved by tumor (%)*	20	(10–30)
Location of tumor		
PZ	45	(95.7)
CZ and/or TZ	0	(0.0)
PZ and TZ	1	(2.1)
Gleason grade group		
No tumor	1	(2.1)
1 (≤ 6)†	2	(4.3)
2 (3 + 4 = 7)†	18	(38.3)
3 (4 + 3 = 7)†	9	(19.1)
4 (8)†	7	(14.9)
5 (≥ 9)†	9	(19.1)
Tumor stage		
No tumor	1	(2.1)
T2a	3	(6.4)
T2b	0	(0.0)
T2c	26	(55.3)
T3/T4	18	(38.3)

Note: Unless otherwise stated, patient numbers are stated in the right column with percentages in parentheses.
Abbreviations: CZ, central zone; PSA, prostate-specific antigen; PZ, peripheral zone; TZ, transition zone.
*Data are medians, with interquartile ranges in parentheses.
†Equivalent Gleason score is shown in parentheses.

3.2 | Sensitivity and Conspicuity

88 tumors were found in 47 prostatectomy specimens by histopathology (Table 3). The sensitivity of the evaluated MRI sequences for detecting PCa lesions is depicted in Figure 2 A. The highest sensitivities were recorded for T2WI (93.5%) and DCE-T1W imaging (82.6%) sequences. Lower sensitivity values were recorded for ADC (63.0%) and DWI (58.7%) sequences.

Tumor localization analysis, comparing mpMRI to pathology, showed two true negatives, six false negatives and two false positives (Table 3). The overall MRI sensitivity for detecting PCa was 93.2% with a positive predictive value of 97.62%. As the evaluation was lesion-based, a negative result for the left or right side of the prostate gland could be assumed only when no single tumor lesion was seen on that side and no tumor extension from the contralateral side. A total of 10 negative results were reported on mpMRI (Table 3). From these, four cases were confirmed as negative on postsurgical pathology and the remaining six cases had a Gleason score of six or seven, the numbers being insufficient for a meaningful statistical analysis.

TABLE 3 | Contingency table for MRI and pathology results.

		Pathology		
		Positive	Negative	Total
MRI	Positive	82	2	84
	Negative	6	4	10
	Total	88	6	94

Abbreviation: MRI, magnetic resonance imaging.

A comparison between the investigational mpMRI and pathology reports also revealed a 74.5% ($n = 35$) concordance in determining the presence or absence of extra-prostatic extension (EPE). Of the remaining 25.5% ($n = 12$) cases, 6.4% ($n = 3$) had microscopic or ≤ 3 mm EPE and 4.3% ($n = 2$) had microscopic bladder neck invasion.

The conspicuity scores for the evaluated sequences are depicted in Figure 2B. The tumor conspicuity was most prominent on T2WI (8.5 ± 0.2) followed by DCE-T1W images (7.9 ± 0.3). Lower values were recorded for ADC (6.2 ± 0.3) and DWI (6.1 ± 0.3). *T*-test analysis showed a statistical significance between higher lesional conspicuity values detected on T2WI compared to DWI ($p < 0.0001$) and ADC images ($p < 0.0001$), and between DCE-T1W imaging compared to DWI ($p = 0.0002$) and ADC images ($p = 0.0007$). No significant difference was noted between lesional conspicuity scores on T2W versus DCE sequences ($p = 0.1510$). Linear correlation analysis for conspicuity scores on each sequence against T2W was also performed. The highest correlation was found between T2W and DCE sequences ($r = 0.55$), followed by DWI ($r = 0.45$), and ADC ($r = 0.31$) sequences. Pearson's correlation coefficient for conspicuity score of each sequence with Gleason grade found on histopathology were as follows: 0.39, 0.33, 0.31, and 0.21 for T2W, DCE, DWI, and ADC, respectively.

The added value of DCE MRI is shown in Figure 3. In 83% of patients DCE imaging increased confidence or was scored essential to tumor detection and localization. An example of mpMRI and whole-mount pathology correlation with differential conspicuity of high-grade PCA on the different MRI acquisition is shown in Figure 4.

3.3 | Image Quality

Figure 5 summarizes the qualitative measures of image quality for each of the mpMRI acquisition sequences by

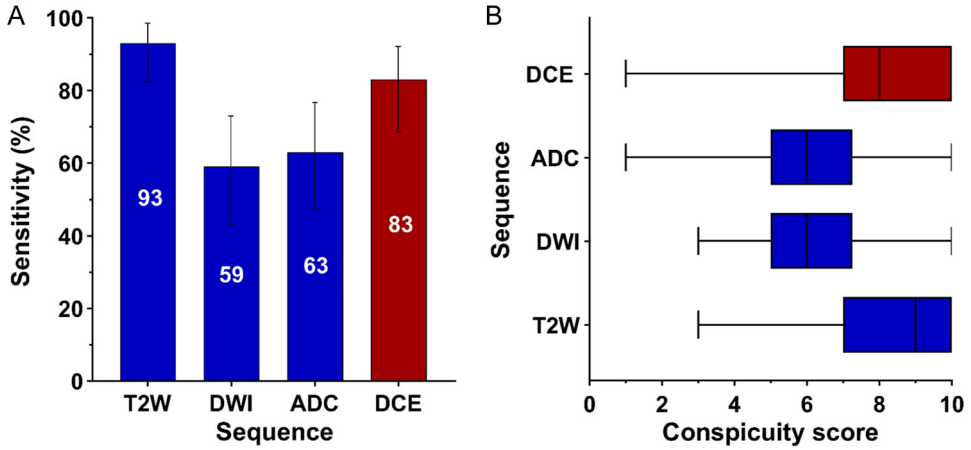

FIGURE 2 | (A) Per lesion sensitivity of MRI sequences compared to whole mount pathology with percentages given above the bars and (B) Box plot of the tumor conspicuity scores for each of the evaluated MRI sequences. [Color figure can be viewed at wileyonlinelibrary.com]

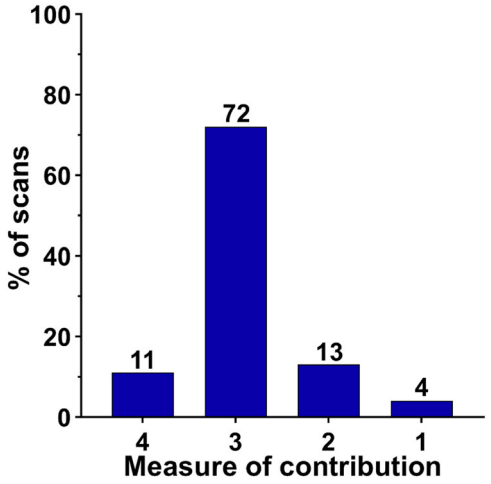

FIGURE 3 | Relative contribution of DCE-T1W MRI in lesion detection. 4 = Essential, 3 = Increased Confidence, 2 = No Added Value, 1 = No DCE. [Color figure can be viewed at wileyonlinelibrary.com]

assigning a score from 1 to 4. T2W images displayed the highest quality, with 98% of scans scored as excellent or satisfactory quality and a mean score of 3.8. A relatively lower quality was recorded for other sequences, with 79% of DWI, 81% of ADC and 77% of DCE images being of excellent or satisfactory quality, and with mean scores of 3.3, 3.4, and 3.0, respectively. Of note is that DCE images were mostly acquired without fat suppression and this factor reduced the score by 1 point for 24 out of 47 studies, even when the image quality remained unaffected.

3.4 | ADC Values and Gleason Score

Table 4 shows the mean ADC values of all the tumors detected on mpMRI, categorized against respective Gleason score and grade group [32]. A negative correlation was observed ($p < 0.0001$), similar to prior reports [36–39].

3.5 | Analyses of the Prospective Clinical mpMRI Reports

The prospective radiology clinical reports were available for all 47 patients in this study for comparison to the over-reads and pathology (Table 5). All 47 reports used a group-standardized reporting system based on PI-RADS v2.1 for anatomical regional localization, and using the T2WI, DWI and ADC maps for the primary scoring. The DCE images, although available, were not emphasized or used universally, as per guidelines. Table 5 shows 42.7% of scans had a significant difference from the over-reads where the DCE images were included in the assessment in every case and where a significance threshold was considered a change in the PI-RADS and/or T-staging. Table 5 categorizes both significant and nonsignificant differences. The most common errors were missed tumors on the contralateral side (12.8% of cases, or 30% of detected errors) and erroneous determination of EPE (14.9% of cases or 35% of detected errors). In each of these cases DCE images were found to be contributory (Figure 3, category 3 or 4).

4 | Discussion

PI-RADS provides a framework for mpMRI scanning and interpretation to achieve standardization. It is evidence-based and dependent on the collective experience of an international group of experts. PI-RADS has evolved with the most recent update published in 2019. The PI-RADS Steering Committee justified a reduced role of DCE-MRI by the lack of expert consensus, stating a difficulty of interpreting DCE-MRI sequences by eye [40]. Alternative methods include the Likert scale [41–43], ESUR score [44], or EPE grade [45, 46]. The Likert scale, proposed in the United Kingdom [41], employs all mpMRI acquisitions with DCE having a primary role for both transitional and peripheral zone cancer [18, 42, 43]. Furthermore, DCE imaging can either upgrade or downgrade the score, whereas in PI-RADS, DCE imaging only upgrades the score in certain

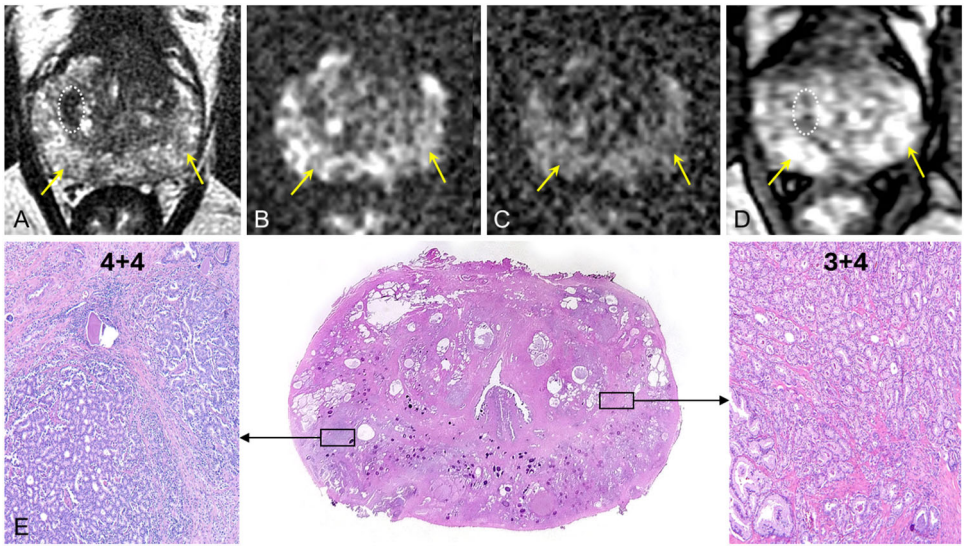

FIGURE 4 | PCa multi-focal scattered lesions in the bilateral peripheral zones (PZs) most conspicuous on T2W and DCE-T1W scans in a 65-year-old male with rising PSA. Axial T2W images (A), DWI with *b*-value of 1600 (B), corresponding ADC map (C), and arterial phase DCE-T1W images (D). Histopathological specimen showing multifocal postero-lateral PZ, with corresponding high magnification of regional highest-grade tumor (E). Spatially corresponding tumor foci (Gleason score 4 + 4 on the right, and 3 + 4 on the left) are marked by yellow arrows (A–D) and black rectangles (E). Focal and nonuniform T2 signal hypo-intensities are evident at the left posterolateral and right lateral PZ (A). DWI and ADC sequences provide lower lesion conspicuity with indistinct signal changes throughout the PZ (B and C). The mean ADC value for the lesion on the left is 1064 mm^2/s and 1186 mm^2/s on the right (C, arrows), which was interpreted as benign (PI-RADS 2) on the prospective clinical radiology report. Combined with the T2W features, the prospective report provided a PI-RADS score of up to 3, based on T2W images. DCE-T1W imaging, however, shows distinct arterial enhancement (D, yellow arrows), in keeping with malignancy. A 1.7 cm confluent area of T2 hypo-intensity (white dotted oval, A and D) was also prospectively reported in the central gland with features of broad internal capsular abutment and possible extra-capsular extension and categorized as a PI-RADS 5 lesion. However, this region was not associated with diffusion restriction (B, C) or early arterial enhancement (D), and, in retrospect, in keeping with central zone (CZ) stromal hypertrophy. Postsurgical pathology revealed left and right PZ acinar adenocarcinoma with a Gleason score of 3 + 4 = 7 and 4 + 4 = 8, respectively, corresponding to T2W and DCE-T1W imaging (A and D). No tumor was identified in the CZ, with histological features of stromal hypertrophy. [Color figure can be viewed at wileyonlinelibrary.com]

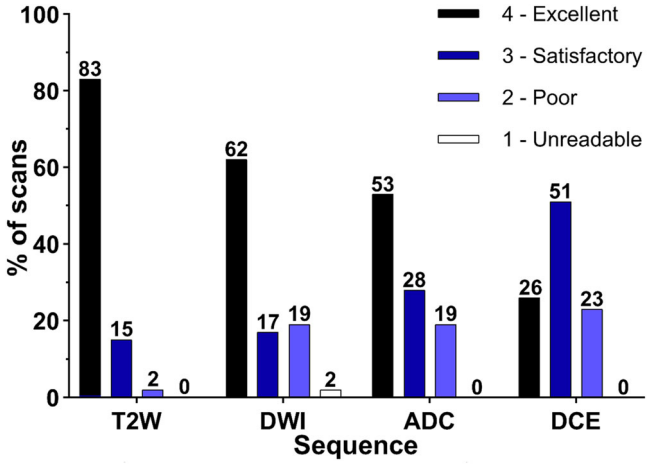

FIGURE 5 | Image quality of sequences analyzed. Image quality is scored from 1 to 4. The relative quality score of T2W images greater than for DWI ($p = 0.0043$), ADC ($p = 0.0007$) or DCE T1W ($p < 0.0001$). A higher proportion of DCE scans were given a score of 3 due to the lack of fat suppression in a subset of cases (Fat-suppression is the current recommended standard of practice by the ACR PI-RADS documentation). [Color figure can be viewed at wileyonlinelibrary.com]

TABLE 4 | ADC values against Gleason groups.

Gleason score	Gleason grade group	Mean ADC value
No tumor	No tumor	956.5
≤ 6	1	823.1
7 = 3 + 4	2	771.4
7 = 4 + 3	3	663.2
8	4	490.4
≥ 9	5	482.9

Abbreviation: ADC, apparent diffusion coefficient.

scenarios [18, 41, 43]. The Prostate Imaging for Recurrence Reporting (PI-RR) is another scoring system, proposed in 2021 by the ESUR and members of the PI-RADS Steering Committee, where DCE imaging is weighted with more significance [18, 47], and studies suggest DCE images generate the highest inter-reader agreement [48, 49].

Our overarching study objective was to assess the relative contributions of the different components of a standardized

TABLE 5 | Classification of interpretation differences on standardized prospective clinical mpMRI.

Classification				Nonsignificant differences ($n = 22$)	n of 22	% of cohort	% of NSDS
Significant differences ($n = 20$)	n of 20	% of cohort	% of SDS				
Under-read differences ($n = 10$)				Transcription error	3	6.4	13.6
Size measurement discrepancy	2	4.3	10	Language ambiguity	5	10.6	22.7
Missed tumor on contralateral side	6	12.8	30	Location discrepancy	5	10.6	22.7
Missed EPE	2	4.3	10	Incorrect/additional diagnosis (e.g., prostatitis)	6	12.8	27.3
Over-read differences ($n = 10$)				Tumor count discrepancy without stage change	2	4.3	4.5
Stromal hypertrophy interpreted as tumor	3	6.4	15	Size measurement discrepancy without stage change	1	2.1	2.3
Erroneous determination of EPE	7	14.9	35				
Total	20	42.7	100	Total	22	46.8	100

Note: Cohort references the total of 47 patients included in this study.
Abbreviations: EPE, extra-prostatic extension; mpMRI, multiparametric magnetic resonance imaging; NSDS, nonsignificant differences; SDS, significant differences.

mpMRI scan, searching for optimization in diagnostic yield. Our results support three main conclusions. First, PI-RADS may be underweighting the role of DCE images. In our study, it was determined that DCE sequences, at minimum, improved diagnostic confidence in most cases (83%) and was essential in 11% of cases, suggesting that employment of DCE images as a major score element would markedly increase PCa PZ lesion detection and staging accuracy.

Second, the role of DWI and derivative ADC mapping is relatively inferior to T2W or DCE imaging for lesion detection, particularly for smaller or multifocal disease. Here, we show that DWI and ADC have significantly lower diagnostic performance compared to T2W and DCE imaging. DWI sequences are intrinsically low signal, noisy, and lower resolution compared to the other scanning techniques. Longer scan times, usually requiring multiples of minutes, leads to motion-related deterioration from patient motion and other internal sources of movement, such as bowel and bladder contractions, or from susceptibility-related signal distortion from adjacent bowel gas.

Third, our study, which examined prospective clinical reports that strictly used the prescribed PI-RADS v2.1 methodology, showed that the most common errors are from under-staging of patients with multi-focal and bilateral disease, where multifocal and contralateral lesions were not appreciated on T2W and DWI-ADC imaging alone and most often scored as borderline PI-RADS 3. The next most common error was EPE under/over-reporting. Our findings show that these errors would be significantly reduced by implementing DCE images.

Prior reports with at least similar sample sizes measured sensitivities from 47.8% to 94% for T2WI and 73% to 82.6% for DCE-MRI [50–52], including higher sensitivity for DCE-MRI versus T2WI in two studies. A meta-analysis involving data extracted from 22 articles involving 1483 patients determined area under the curve values of 0.82, 0.81, 0.7 and 0.83 and sensitivity values of 55%, 46%, 46%, and 64% for DCE-MRI, DWI, T2WI, and combined T2WI and DCE-MRI, respectively [2]. In keeping with our findings, DCE scans have been shown to improve detection of small tumors or tumors in cases with technically impaired T2W/DWI scans [18, 53].

Our results have several other implications. There is active development for further improving standardized reporting with computational image analysis using Artificial Intelligence (AI). The use of DCE scans should be considered, along with T2WI and DWI, for neural-network training and development of AI-based computer-assisted diagnostics and it would be important to include annotated DCE images. Further gains will also result from focused development and improvement in DCE scanning. Newer techniques may include radial stack-of-stars combined with neural-network implementations useful for reducing noise, improving speed and resolution, and eliminating artifacts [54].

Limitations of our study include a retrospective partially-blinded design, with case review conducted knowing patients had PCa and introducing bias for sensitivity. While a fully blinded prospective analysis, including patients without PCa, would provide another measure of sensitivity and specificity,

our study was designed to compare the performance of different scan techniques. We achieved that by comparing a per-lesion detection in total prostatectomy patients with spatial mapping to the whole mount pathology. Another concern may be that our measure of DWI inferiority may be the result of poor techniques. To test that, we compared the ADC quantitative map of tumor lesions to the Gleason Score, showing that there was an inverse correlation between these measures. This is supported by prior reports and provides indirect evidence that our DWI and ADC maps are behaving as expected.

5 | Conclusions

DCE sequences have marked potential for improving PCa diagnosis, with unique information related to perfusion and tumor neovascularization. We show DCE imaging improved diagnostic performance of mpMRI, using whole gland pathology for reference, and generated higher staging accuracy on TNM classification. A reporting system for mpMRI should assign DCE imaging similar weighting and importance as T2W images.

Acknowledgments

The authors would like to express our sincere thanks to Richard Sucgang, PhD, Faculty Development and Tariq Nisar, MPH, Senior Data Scientist at the Center for Health Data Science & Analytics, Houston Methodist Research Institute for their support with statistical analysis of data. NIH 1R01CA245920-02. MD Anderson Foundation. Houston Methodist Neal Cancer Center.

Ethics Statement

Study performed on patient data with Institutional Review Borad approval with a waiver for informed consent.

Conflicts of Interest

The authors declare no conflicts of interest.

Data Availability Statement

The data underlying this article will be shared on reasonable request to the corresponding author.

References

1. M. A. Bjurlin, P. R. Carroll, S. Eggener, et al., "Update of the Standard Operating Procedure on the Use of Multiparametric Magnetic Resonance Imaging for the Diagnosis, Staging and Management of Prostate Cancer," *Journal of Urology* 203, no. 4 (2020): 706–712, https://doi.org/10.1097/JU.0000000000000617.

2. C. H. Tan, B. Paul Hobbs, W. Wei, and V. Kundra, "Dynamic Contrast-Enhanced MRI for the Detection of Prostate Cancer: Meta-Analysis," *American Journal of Roentgenology* 204, no. 4 (2015): W439–W448, https://doi.org/10.2214/AJR.14.13373.

3. A. A. Tavakoli, T. Hielscher, P. Badura, et al., "Contribution of Dynamic Contrast-Enhanced and Diffusion MRI to PI-RADS for Detecting Clinically Significant Prostate Cancer," *Radiology* 306, no. 1 (2023): 186–199, https://doi.org/10.1148/radiol.212692.

4. American College of Radiology. PI-RADS Version 2.1. Prostate Imaging-Reporting and Data System. Published 2019, http://www.acr.org/~/media/ACR/Documents/PDF/QualitySafety/Resources/PIRADS/PIRADS.

5. American Urological Association, Standard Operating Procedure for Multiparametric Magnetic Resonance Imaging in the Diagnosis, Staging and Management of Prostate Cancer, Standard Operating Procedure for Multiparametric Magnetic Resonance Imaging in the Diagnosis, Staging and Management of Prostate Cancer, https://www.auanet.org/guidelines-and-quality/guidelines/other-clinical-guidance/mri-of-the-prostate-sop.

6. S. Verma, B. Turkbey, N. Muradyan, et al., "Overview of Dynamic Contrast-Enhanced MRI in Prostate Cancer Diagnosis and Management," *American Journal of Roentgenology* 198, no. 6 (2012): 1277–1288, https://doi.org/10.2214/AJR.12.8510.

7. A. Villers, P. Puech, D. Mouton, X. Leroy, C. Ballereau, and L. Lemaitre, "Dynamic Contrast Enhanced, Pelvic Phased Array Magnetic Resonance Imaging of Localized Prostate Cancer for Predicting Tumor Volume: Correlation With Radical Prostatectomy Findings," *Journal of Urology* 176, no. 6 Pt 1 (2006): 2432–2437, https://doi.org/10.1016/j.juro.2006.08.007.

8. M. Abramson, M. DeMasi, D. Zhu, et al., "Biparametric Versus Multiparametric MRI for the Detection of Clinically Significant Prostate Cancer in a Diverse, Multiethnic Population," *Abdominal Radiology* 49, no. 7 (2024): 2491–2498, https://doi.org/10.1007/s00261-024-04332-6.

9. J. Dana, C. Reinhold, and S. Gauvin, "Is PI-RADS Ready for Biparametric Prostate Mri?," *American Journal of Roentgenology* 222, no. 5 (2024): e2431094, https://doi.org/10.2214/AJR.24.31094.

10. M. Uyanik, H. T. Vigneswaran, G. R. Hale, P. Gann, R. Magin, and M. R. Abern, "Biparametric Quantitative MRI for Prostate Cancer Detection," *Topics in Magnetic Resonance Imaging* 32, no. 6 (2023): 66–72, https://doi.org/10.1097/RMR.0000000000000308.

11. R. Iacob, E. R. Stoicescu, S. Cerbu, D. L. Manolescu, R. Bardan, and A. Cumpănaş, "Could Biparametric MRI Replace Multiparametric MRI in the Management of Prostate Cancer?," *Life* 13, no. 2 (2023): 465, https://doi.org/10.3390/life13020465.

12. M. J. Belue, E. C. Yilmaz, A. Daryanani, and B. Turkbey, "Current Status of Biparametric MRI in Prostate Cancer Diagnosis: Literature Analysis," *Life* 12, no. 6 (2022): 804, https://doi.org/10.3390/life12060804.

13. G. Brembilla, F. Giganti, H. Sidhu, et al., "Diagnostic Accuracy of Abbreviated Bi-Parametric MRI (A-bpMRI) for Prostate Cancer Detection and Screening: A Multi-Reader Study," *Diagnostics* 12, no. 2 (2022): 231, https://doi.org/10.3390/diagnostics12020231.

14. K. K. Porter, A. King, S. J. Galgano, R. L. Sherrer, J. B. Gordetsky, and S. Rais-Bahrami, "Financial Implications of Biparametric Prostate MRI," *Prostate Cancer and Prostatic Diseases* 23, no. 1 (2020): 88–93, https://doi.org/10.1038/s41391-019-0158-x.

15. H. M. Reynolds, S. Tadimalla, Y. F. Wang, et al., "Semi-Quantitative and Quantitative Dynamic Contrast-Enhanced (DCE) MRI Parameters as Prostate Cancer Imaging Biomarkers for Biologically Targeted Radiation Therapy," *Cancer Imaging: The Official Publication of the International Cancer Imaging Society* 22, no. 1 (2022): 71, https://doi.org/10.1186/s40644-022-00508-9.

16. A. D. J. Baur, J. Schwabe, J. Rogasch, et al., "A Direct Comparison of Contrast-Enhanced Ultrasound and Dynamic Contrast-Enhanced Magnetic Resonance Imaging for Prostate Cancer Detection and Prediction of Aggressiveness," *European Radiology* 28, no. 5 (2018): 1949–1960, https://doi.org/10.1007/s00330-017-5192-2.

17. M. Gatti, R. Faletti, G. Calleris, et al., "Prostate Cancer Detection With Biparametric Magnetic Resonance Imaging (bpMRI) by Readers With Different Experience: Performance and Comparison With Multiparametric (Mpmri)," *Abdominal Radiology* 44, no. 5 (2019): 1883–1893, https://doi.org/10.1007/s00261-019-01934-3.

18. S. Guljaš, Z. Dupan Krivdić, M. Drežnjak Madunić, et al., "Dynamic Contrast-Enhanced Study in the mpMRI of the Prostate—Unnecessary

or Underutilised? A Narrative Review," *Diagnostics* 13, no. 22 (2023): 3488, https://doi.org/10.3390/diagnostics13223488.

19. B. Turkbey and A. S. Purysko, "PI-RADS: Where Next," *Radiology* 307, no. 5 (2023): e223128, https://doi.org/10.1148/radiol.223128.

20. K. M. Koch, S. Bhave, A. Gaddipati, et al., "Multispectral Diffusion-Weighted Imaging Near Metal Implants," *Magnetic Resonance in Medicine* 79, no. 2 (2018): 987–993, https://doi.org/10.1002/mrm.26737.

21. J. P. Neri, M. F. Koff, K. M. Koch, and E. T. Tan, "Validating the Accuracy of Multispectral Metal Artifact Suppressed Diffusion-Weighted Imaging," *Medical Physics* 49, no. 10 (2022): 6538–6546, https://doi.org/10.1002/mp.15925.

22. M. Bekiesińska-Figatowska, "Artifacts in Magnetic Resonance Imaging," *Polish Journal of Radiology* 80 (2015): 93–106, https://doi.org/10.12659/PJR.892628.

23. Y. Mazaheri, H. A. Vargas, G. Nyman, O. Akin, and H. Hricak, "Image Artifacts on Prostate Diffusion-Weighted Magnetic Resonance Imaging," *Academic Radiology* 20, no. 8 (2013): 1041–1047, https://doi.org/10.1016/j.acra.2013.04.005.

24. J. Abreu-Gomez, C. Lim, G. O. Cron, S. Krishna, N. Sadoughi, and N. Schieda, "Pharmacokinetic Modeling of Dynamic Contrast-Enhanced (DCE)-MRI in PI-RADS Category 3 Peripheral Zone Lesions: Preliminary Study Evaluating DCE-MRI as an Imaging Biomarker for Detection of Clinically Significant Prostate Cancers," *Abdominal Radiology* 46, no. 9 (2021): 4370–4380, https://doi.org/10.1007/s00261-021-03035-6.

25. S. Afshari Mirak, A. Mohammadian Bajgiran, K. Sung, et al., "Dynamic Contrast-Enhanced (DCE) MR Imaging: The Role of Qualitative and Quantitative Parameters for Evaluating Prostate Tumors Stratified by Gleason Score and PI-RADS V2," *Abdominal Radiology* 45, no. 7 (2020): 2225–2234, https://doi.org/10.1007/s00261-019-02234-6.

26. G. Cristel, A. Esposito, A. Damascelli, et al., "Can DCE-MRI Reduce the Number of PI-RADS v.2 False Positive Findings? Role of Quantitative Pharmacokinetic Parameters in Prostate Lesions Characterization," *European Journal of Radiology* 118 (2019): 51–57, https://doi.org/10.1016/j.ejrad.2019.07.002.

27. M. Taghipour, A. Ziaei, F. Alessandrino, et al., "Investigating the Role of DCE-MRI, Over T2 and DWI, in Accurate PI-Rads v2 Assessment of Clinically Significant Peripheral Zone Prostate Lesions as Defined at Radical Prostatectomy," *Abdominal Radiology* 44, no. 4 (2019): 1520–1527, https://doi.org/10.1007/s00261-018-1807-6.

28. C. W. Yuan, R. Li, Z. H. Li, et al., "[Application of Dynamic Contrast Enhanced Status in Multiparametric Magnetic Resonance Imaging for Prostatic Cancer with PI-RADS 4 Lesion]," *Beijing da xue xue bao. Yi xue ban = Journal of Peking University. Health Sciences* 55, no. 5 (2023): 838–842, https://doi.org/10.19723/j.issn.1671-167X.2023.05.010.

29. F. B. Franco and F. M. Fennessy, "Arguments Against Using an Abbreviated or Biparametric Prostate MRI Protocol," *Abdominal Radiology* 45, no. 12 (2020): 3982–3989, https://doi.org/10.1007/s00261-020-02474-x.

30. P. F. Fulgham, D. B. Rukstalis, I. B. Turkbey, et al., "AUA Policy Statement on the Use of Multiparametric Magnetic Resonance Imaging in the Diagnosis, Staging and Management of Prostate Cancer," *Journal of Urology* 198, no. 4 (2017): 832–838, https://doi.org/10.1016/j.juro.2017.04.101.

31. A. M. Hötker, H. A. Vargas, and O. F. Donati, "Abbreviated MR Protocols in Prostate MRI," *Life* 12, no. 4 (2022): 552, https://doi.org/10.3390/life12040552.

32. J. I. Epstein, L. Egevad, M. B. Amin, B. Delahunt, J. R. Srigley, and P. A. Humphrey, "The 2014 International Society of Urological Pathology (ISUP) Consensus Conference on Gleason Grading of Prostatic Carcinoma: Definition of Grading Patterns and Proposal for a New Grading System," *American Journal of Surgical Pathology* 40, no. 2 (2016): 244–252, https://doi.org/10.1097/PAS.0000000000000530.

33. G. J. L. H. van Leenders, T. H. van der Kwast, D. J. Grignon, et al., "The 2019 International Society of Urological Pathology (ISUP) Consensus Conference on Grading of Prostatic Carcinoma," *American Journal of Surgical Pathology* 44, no. 8 (2020): e87–e99, https://doi.org/10.1097/PAS.0000000000001497.

34. M. K. Buyyounouski, P. L. Choyke, J. K. McKenney, et al., "Prostate Cancer - Major Changes in the American Joint Committee on Cancer Eighth Edition Cancer Staging Manual," *CA: A Cancer Journal for Clinicians* 67, no. 3 (2017): 245–253, https://doi.org/10.3322/caac.21391.

35. American Cancer Society. Prostate Cancer Stages, https://www.cancer.org/cancer/types/prostate-cancer/detection-diagnosis-staging/staging.html.

36. R. Manetta, P. Palumbo, C. Gianneramo, et al., "Correlation Between ADC Values and Gleason Score in Evaluation of Prostate Cancer: Multicentre Experience and Review of the Literature," *Gland Surgery* 8, no. Suppl 3 (2019): S216–S222, https://doi.org/10.21037/gs.2019.05.02.

37. S. Woo, S. Y. Kim, J. Y. Cho, and S. H. Kim, "Preoperative Evaluation of Prostate Cancer Aggressiveness: Using ADC and ADC Ratio in Determining Gleason Score," *American Journal of Roentgenology* 207, no. 1 (2016): 114–120, https://doi.org/10.2214/AJR.15.15894.

38. F. De Cobelli, S. Ravelli, A. Esposito, et al., "Apparent Diffusion Coefficient Value and Ratio as Noninvasive Potential Biomarkers to Predict Prostate Cancer Grading: Comparison With Prostate Biopsy and Radical Prostatectomy Specimen," *American Journal of Roentgenology* 204, no. 3 (2015): 550–557, https://doi.org/10.2214/AJR.14.13146.

39. J. Nowak, U. Malzahn, A. D. Baur, et al., "The Value of ADC, T2 Signal Intensity, and a Combination of Both Parameters to Assess Gleason Score and Primary Gleason Grades in Patients With Known Prostate Cancer," *Acta Radiologica* 57, no. 1 (2016): 107–114, https://doi.org/10.1177/0284185114561915.

40. N. A. Parra, A. Pollack, F. M. Chinea, et al., "Automatic Detection and Quantitative DCE-MRI Scoring of Prostate Cancer Aggressiveness," *Frontiers in Oncology* 7 (2017): 259, https://doi.org/10.3389/fonc.2017.00259.

41. National Institute for Health and Care Excellence. Prostate Cancer: Diagnosis and Management. Published 2019, https://www.nice.org.uk/guidance/ng131/evidence/d-diagnosing-and-identifying-clinicallysignificant-prostate-cancer-pdf-6779081777.

42. M. Peters, D. Eldred-Evans, P. Kurver, et al., "Predicting the Need for Biopsy to Detect Clinically Significant Prostate Cancer in Patients with a Magnetic Resonance Imaging-Detected Prostate Imaging Reporting and Data System/Likert ≥3 Lesion: Development and Multinational External Validation of the I," *European Urology* 82, no. 5 (2022): 559–568, https://doi.org/10.1016/j.eururo.2022.07.022.

43. A. Latifoltojar, M. B. Appayya, T. Barrett, and S. Punwani, "Similarities and Differences Between Likert and PIRADS v2.1 Scores of Prostate Multiparametric MRI: A Pictorial Review of Histology-Validated Cases," *Clinical Radiology* 74, no. 11 (2019): 895.e1–895.e15, https://doi.org/10.1016/j.crad.2019.08.020.

44. J. O. Barentsz, J. Richenberg, R. Clements, et al., "ESUR Prostate MR Guidelines 2012," *European Radiology* 22, no. 4 (2012): 746–757, https://doi.org/10.1007/s00330-011-2377-y.

45. S. Mehralivand, J. H. Shih, S. Harmon, et al., "A Grading System for the Assessment of Risk of Extraprostatic Extension of Prostate Cancer at Multiparametric MRI," *Radiology* 290, no. 3 (2019): 709–719, https://doi.org/10.1148/radiol.2018181278.

46. U. Asfuroğlu, B. B. Asfuroğlu, H. Özer, et al., "Which One Is Better for Predicting Extraprostatic Extension on Multiparametric MRI: ESUR Score, Likert Scale, Tumor Contact Length, or EPE Grade?," *European Journal of Radiology* 149 (2022): 110228, https://doi.org/10.1016/j.ejrad.2022.110228.

47. V. Panebianco, G. Villeirs, J. C. Weinreb, et al., "Prostate Magnetic Resonance Imaging for Local Recurrence Reporting (PI-RR): International Consensus -Based Guidelines on Multiparametric Magnetic Resonance Imaging for Prostate Cancer Recurrence after Radiation Therapy and Radical Prostatectomy," *European Urology Oncology* 4, no. 6 (2021): 868–876, https://doi.org/10.1016/j.euo.2021.01.003.

48. C. Bergaglio, V. Giasotto, M. Marcenaro, et al., "The Role of mpMRI in the Assessment of Prostate Cancer Recurrence Using the PI-RR System: Diagnostic Accuracy and Interobserver Agreement in Readers With Different Expertise," *Diagnostics* 13, no. 3 (2023): 387, https://doi.org/10.3390/diagnostics13030387.

49. O. Rouvière, O. Valette, S. Grivolat, et al., "Recurrent Prostate Cancer After External Beam Radiotherapy: Value of Contrast-Enhanced Dynamic MRI in Localizing Intraprostatic Tumor–Correlation With Biopsy Findings," *Urology* 63, no. 5 (2004): 922–927, https://doi.org/10.1016/j.urology.2003.12.017.

50. I. Ocak, M. Bernardo, G. Metzger, et al., "Dynamic Contrast-Enhanced MRI of Prostate Cancer at 3 T: A Study of Pharmacokinetic Parameters," *American Journal of Roentgenology* 189, no. 4 (2007): W192–W201, https://doi.org/10.2214/AJR.06.1329.

51. C. K. Kim, "Prostate Imaging Reporting and Data System (PI-RADS) V 2.1: Overview and Critical Points," *Journal of the Korean Society of Radiology* 84, no. 1 (2023): 75–91, https://doi.org/10.3348/jksr.2022.0169.

52. A. B. Cheikh, N. Girouin, M. Colombel, et al., "Evaluation of T2-Weighted and Dynamic Contrast-Enhanced MRI in Localizing Prostate Cancer Before Repeat Biopsy," *European Radiology* 19, no. 3 (2009): 770–778, https://doi.org/10.1007/s00330-008-1190-8.

53. A. Chatterjee, S. Tokdemir, A. J. Gallan, et al., "Multiparametric MRI Features and Pathologic Outcome of Wedge-Shaped Lesions in the Peripheral Zone on T2-Weighted Images of the Prostate," *American Journal of Roentgenology* 212, no. 1 (2019): 124–129, https://doi.org/10.2214/AJR.18.19742.

54. Z. Fu, S. Mandava, M. B. Keerthivasan, et al., "A Multi-Scale Residual Network for Accelerated Radial MR Parameter Mapping," *Magnetic Resonance Imaging* 73 (2020): 152–162, https://doi.org/10.1016/j.mri.2020.08.013.